CORE
Metadata, citation and similar papers at core.ac.uk
Provided by Explore Bristol Research

Bryant, S. M., Kong, C. H. T., Cannell, M. B., Orchard, C. H., & James, A. F. (2018). Loss of caveolin-3-dependent regulation of I_{Ca} in rat ventricular myocytes in heart failure. *AJP - Heart and Circulatory Physiology*, *314*(3), H521-H529. https://doi.org/10.1152/ajpheart.00458.2017, https://doi.org/10.1152/ajpheart.00458.2017

Peer reviewed version

Link to published version (if available):
10.1152/ajpheart.00458.2017
10.1152/ajpheart.00458.2017

Link to publication record in Explore Bristol Research
PDF-document

This is the author accepted manuscript (AAM). The final published version (version of record) is available online via APS journal at http://ajpheart.physiology.org/content/early/2017/11/03/ajpheart.00458.2017. Please refer to any applicable terms of use of the publisher.

University of Bristol - Explore Bristol Research

General rights

This document is made available in accordance with publisher policies. Please cite only the published version using the reference above. Full terms of use are available:
http://www.bristol.ac.uk/pure/about/ebr-terms

Loss of caveolin-3-dependent regulation of I_{Ca} in rat ventricular myocytes in heart failure

Simon M. Bryant, PhD, Cherrie H.T. Kong, PhD, Mark B. Cannell, PhD, FRSNZ, Clive H. Orchard, PhD, DSc, FRSB, Andrew F. James*, DPhil,

School of Physiology, Pharmacology and Neuroscience,
Biomedical Sciences Building,
University of Bristol,
Bristol, BS8 1TD,
UK

*Corresponding author:
E-mail: a.james@bristol.ac.uk,
Telephone: +44-(0)-117-331-2297. Orcid id: orcid.org/0000-0002-2035-9489

Running title: Loss of caveolin-3 regulation of I_{Ca} in heart failure

ABSTRACT

β_2-adrenoceptors and the L-type Ca current (I_{Ca}) redistribute from the t-tubules to the surface membrane of ventricular myocytes from failing hearts. The present study investigated the role of changes in caveolin-3 (Cav-3) and protein kinase A (PKA) signaling, both of which have previously been implicated in this redistribution. I_{Ca} was recorded using the whole cell patch clamp technique from ventricular myocytes isolated from the hearts of rats that had undergone either coronary artery ligation (CAL) or equivalent Sham operation 18 weeks earlier. I_{Ca} distribution between the surface and t-tubule membranes was determined using formamide-induced detubulation (DT). In Sham myocytes, β_2-adrenoceptor stimulation increased I_{Ca} in intact, but not DT myocytes; however, forskolin (to increase cAMP directly) and H-89 (to inhibit PKA) increased and decreased, respectively, I_{Ca} at both the surface and t-tubule membranes. C3SD peptide (which decreases binding to Cav-3) inhibited I_{Ca} in intact but not DT myocytes, but had no effect in the presence of H-89. In contrast, in CAL myocytes, β_2-adrenoceptor stimulation increased I_{Ca} in both intact and DT myocytes, but C3SD had no effect on I_{Ca}; forskolin and H-89 had similar effects as in Sham myocytes. These data show redistribution of β_2-adrenoceptor activity and I_{Ca} in CAL myocytes, and suggest constitutive stimulation of I_{Ca} by PKA in Sham myocytes via concurrent Cav-3-dependent (at the t-tubules) and Cav-3-independent mechanisms, with the former being lost in CAL myocytes.

(230 words)

NEW AND NOTEWORTHY

In ventricular myocytes from normal hearts, regulation of the L-type Ca^{2+} current by β_2-adrenoceptors and the constitutive regulation by caveolin-3 is localized to the t-tubules. In heart failure, the regulation of L-type Ca^{2+} current by β_2-adrenoceptors is redistributed to the surface membrane and the constitutive regulation by caveolin-3 is lost.

INTRODUCTION

The L-type Ca^{2+} current (I_{Ca}) plays a key role in excitation-contraction (EC) coupling in cardiac ventricular myocytes: activation of L-type Ca^{2+} channels (LTCCs) during the action potential causes influx of Ca^{2+} that triggers Ca^{2+} release via ryanodine receptors (RyRs) in the adjacent sarcoplasmic reticulum (SR) membrane (2, 8). Previous work has shown that the function of many of the key proteins involved in EC coupling, including the LTCCs and RyRs, occurs predominantly at the t-tubules: invaginations of the surface membrane which enable near-synchronous SR Ca^{2+} release, and thus contraction, throughout the cell (18, 21, 28). The mechanism for the localization of I_{Ca} at the t-tubules is less clear, although it has been suggested that the caveolar protein, caveolin-3 (Cav-3) plays a role in the localization of I_{Ca}, possibly via a mechanism involving cyclic AMP/protein kinase A (PKA) signaling pathways (1, 5, 9, 24).

Cav-3 is also involved in the localization of cyclic AMP signaling via β_2-adrenoceptors to the t-tubules and it has been proposed that LTCC and β_2-adrenoceptors are co-localized in a Cav-3 signaling microdomain (1, 5, 7, 23, 30). It has been shown that Cav-3 plays a critical role in the constitutive maintenance of I_{Ca} at the t-tubule (5). In heart failure, there is redistribution of β_2 adrenoceptors from the t-tubular to the surface membrane, so that they become more uniformly distributed across the cell membrane (22, 27). This redistribution is associated with a change from localized to more diffuse signaling in response to β_2 adrenergic stimulation (27). We have recently shown in a coronary artery ligation (CAL) model in rat, that ventricular I_{Ca} is also redistributed from the t-tubules to the surface sarcolemma in heart failure (6).

We hypothesize that the redistribution of I_{Ca} following CAL is due to loss of Cav-3 dependent localization at the t-tubules, which may be secondary to the decreased expression of Cav-3 observed in HF. Thus, changes in the localization of the β_2 signaling pathway in

93 heart failure may be associated with a loss of constitutive regulation of I_{Ca} by PKA at the t-
94 tubules. We have, therefore, investigated further the relationship between the distribution of
95 I_{Ca} and changes in Cav-3/β_2 adrenergic signaling observed following CAL in rats (6).
96

METHODS

Animals and surgical procedures

All procedures were performed in accordance with UK legislation and approved by the University of Bristol Ethics Committee. The study was conducted in parallel with other investigations using cells from the same animals to investigate ventricular and atrial cellular remodeling in heart failure and thereby conformed to the reduction component of the 3Rs (3, 6, 16). Adult male Wistar rats (~250 g) were subject to either ligation of the left anterior descending coronary artery (CAL – 10 animals) or equivalent surgery without ligation (Sham – 12 animals). Operations were conducted under general anesthesia (ketamine 75 mg/kg, medetomidine 0.5 mg/kg, i.p.) with appropriate analgesia (buprenorphine 0.05 mg/kg, s.c.), as described previously (6). Data regarding changes in cardiac morphology and function, and in cell morphology, in these groups of animals have been published previously (3, 6).

Myocyte isolation

Left ventricular myocytes were isolated from the hearts ~18 weeks following surgery as described previously (5). Animals were killed under pentobarbitone anesthesia, the heart quickly excised, and Langendorff-perfused at 8 mL/min (37ºC), initially with Tyrode's solution (see below) plus 0.75 mmol/L $CaCl_2$ for 4 minutes, then nominally Ca-free for 4 minutes, and finally plus 1 mg/mL collagenase (Worthington Corp) for 10 minutes. The left ventricle was then excised and shaken in collagenase-containing solution at 37 ºC for 5-7 minutes, filtered, and centrifuged. The supernatant was discarded and the pellet re-suspended in Kraftbrühe solution and stored at 4 °C for 2 - 10 h before use on the day of isolation (20). Detubulation (DT) of myocytes (physical and functional uncoupling of the t-tubules from the surface membrane) was achieved using formamide-induced osmotic shock, as described previously (21).

Solutions

Tyrode's solution for cell isolation contained (in mmol/L): 130 NaCl, 5.4 KCl, 0.4 NaH_2PO_4, 4.2 HEPES, 10 glucose, 1.4 $MgCl_2$, 20 taurine, 10 creatinine, pH 7.4 (NaOH). The KB solution for cell storage contained (in mmol/L): 90 L-glutamic acid, 30 KCl, 10 HEPES, 1 EGTA, 5 Na pyruvate, 20 taurine, 20 glucose, 5 $MgCl_2$, 5 succinic acid, 5 creatine, 2 Na_2ATP and 5 β–OH butyric acid; pH 7.4 with KOH. For patch-clamp experiments, cells were superfused with a solution that contained (in mmol/L): 133 NaCl, 1 $MgSO_4$, 1 $CaCl_2$, 1 Na_2HPO_4, 10 glucose, 10 HEPES, pH 7.4 (NaOH); 5 CsCl was added to inhibit K currents. The pipette solution contained (in mmol/L): 110 CsCl, 20 TEACl, 0.5 $MgCl_2$, 5 Mg-ATP, 5 BAPTA, 10 HEPES, 0.4 GTP-Tris, pH 7.2 (CsOH); BAPTA was used to inhibit Ca-dependent inactivation of I_{Ca}.(33)

Selective β_2-adrenoceptor stimulation was achieved as described previously (5) using the β_2-adrenoceptor agonist zinterol (1 and 3 μmol/L) in the presence of the β_1-adrenoceptor-selective antagonist, atenolol (10 μmol/L); cells were superfused with atenolol alone for at least 4 min prior to superfusion with zinterol in the presence of atenolol. Under these conditions, the effects of 1 and 3 μmol/L zinterol could be completely abolished by 100 nM ICI 118,551, a β_2-adrenoceptor-selective antagonist (5). The plant alkaloid, forskolin (10 μmol/L) was used to activate adenylyl cyclase directly (31). C3SD, a short peptide encompassing the Cav-3 scaffolding domain, was used to disrupt binding of Cav-3 to its protein partners as described previously (5, 13, 15, 23); myocytes were incubated in 1 μmol/L TAT-C3SD for at least 45 minutes before use. PKA was inhibited using H-89 (20 μmol/L) (11, 17).

Recording and analysis of I_{Ca}

Myocytes were placed in a chamber mounted on a Nikon Diaphot inverted microscope. Membrane currents and cell capacitance were recorded using the whole-cell patch-clamp technique, using an Axopatch 200B, Digidata 1322A A/D converter and pClamp 10 (Axon Instruments). Pipette resistance was typically 2-4 MΩ when filled with pipette solution, and pipette capacitance and series resistance were compensated by ~70%. Currents were activated from a holding potential of -80 mV by a 100 ms step depolarization to –40 mV (to inactivate the sodium current, I_{Na}) followed by steps to potentials between -50 and +80 mV for 500 ms, before repolarization to the holding potential, at a frequency of 0.2 Hz. I_{Ca} amplitude (pA) was measured as the difference between peak inward current and current at the end of the depolarizing pulse, and was normalized to cell capacitance (pF; a function of membrane area (25)) to calculate I_{Ca} density (pA/pF). Surface membrane current density was obtained from currents measured in DT myocytes, while t-tubular membrane current density was calculated by subtraction of surface from whole-cell currents and corrected for incomplete DT as described previously (5, 6, 19, 21). DT efficiency, measured from images of intact and DT cells stained with di-8-ANEPPS, was ~84%, and was not different between WT and CAL myocytes (6). To correct for incomplete detubulation, the distribution of membrane capacitance and I_{Ca} between the t-tubule and surface membrane was calculated as described previously (6). As we have reported previously, there was no statistically significant difference between Sham and CAL myocytes in the degree of osmotic shock-induced detubulation, nor was there any relationship between the whole-cell capacitance and the time of recording (6).

Statistics

Data are expressed as mean ± SEM of n myocytes. Statistical analysis was performed using GraphPad Prism (GraphPad Software Inc.). I_{Ca} density-voltage relationship curves were analysed using repeated measures (RM) ANOVA with voltage and corresponding intervention (i.e. DT, H-89 or C3SD) as factors; I_{Ca} properties elicited by a step depolarization to a single voltage were analyzed by 2-way ANOVA; *post hoc* tests used Bonferroni correction. The limit of statistical confidence was taken as $p<0.05$. The errors in derived variables (specifically I_{Ca} density at the t-tubule membrane), and the subsequent statistical analysis (unpaired Student's t-test) were calculated using propagation of errors from the source measurements (6, 14).

RESULTS

The effect of CAL on the response to β_2-adrenoceptor stimulation.

In intact ventricular myocytes from Sham hearts, selective activation of β_2-adrenoceptors (1 and 3 μmol/L zinterol in the presence of 10 μmol/L atenolol) caused a significant, concentration-dependent, increase of I_{Ca}, which reached ~140% of control in the steady-state in the presence of 3 μmol/L of the β_2-agonist (Figs. 1A, left panel, 1B and 1C). In contrast, in detubulated (DT) cells 3 μmol/L zinterol did not increase I_{Ca} (Figs. 1A, right panel, 1B and 1C). In CAL myocytes, 3 μmol/L zinterol caused an increase of ~40% in intact cells and ~29% in DT myocytes (Fig. 1 D – F). Thus, because I_{Ca} recorded in DT cell represents the current at the surface membrane, it appears that in Sham myocytes, the response of I_{Ca} to β_2-adrenoceptor stimulation occurs predominantly at the t-tubule membrane. However, following CAL the β_2-adrenergic response redistributes, and occurs at both the cell surface and t-tubule membranes. These data also show that the DT procedure *per se* is not responsible for the lack of response to zinterol observed in Sham myocytes.

The effect of CAL on the response to forskolin

To investigate whether the distribution of the β_2-adrenergic response was due to the localization of a downstream component of the signaling pathway, we used forskolin (10 μmol/L) to activate adenylyl cyclase directly, to increase cyclic AMP in the absence of adrenoceptor stimulation. Superfusion with forskolin (10 μmol/L) increased I_{Ca} in both intact and DT myocytes from Sham hearts (Fig. 2A). The corresponding mean I_{Ca} density-voltage relationships for intact and DT myocytes are shown in Figure 2B. Figure 2C summarizes the effect of forskolin on I_{Ca} density at a test potential of -10 mV in Sham intact and DT myocytes. Forskolin also caused an increase in I_{Ca} in both intact and DT myocytes from CAL hearts (Figs. 2 D – F). These data show that the increase in I_{Ca} in response to forskolin is

similar in intact Sham and CAL myocytes. More importantly, these data also show that forskolin caused a significant increase in the amplitude of I_{Ca} in DT Sham myocytes, which was similar to that observed in DT CAL myocytes. Thus, it appears that adenylyl cyclase and PKA are present at both the surface and t-tubule membranes in both Sham and CAL myocytes, and can stimulate I_{Ca} to a similar extent at either site. It is unlikely therefore that the lack of effect of zinterol in DT Sham myocytes was due to absence of the components of the cyclic AMP signaling pathway (i.e. adenylyl cyclase and PKA) at the cell surface, but may be due to the absence of β_2-adrenoreceptors.

The effect of CAL on the response to C3SD

Since Cav-3 has been implicated in the localization of β_2-adrenoceptor/cyclic AMP signaling at the t-tubules, we investigated the effect of acutely inhibiting Cav-3 binding to its partner proteins by pretreatment of cells with the C3SD peptide (5, 15). I_{Ca} density was reduced in intact Sham myocytes treated with the C3SD peptide (Figs. 3A left-hand panel, and 3B). However, treatment with C3SD had no effect on I_{Ca} density in DT Sham myocytes (Figs. 3A right panel, and 3C). The effects of treatment with C3SD on I_{Ca} density at 0 mV in intact and DT myocytes from Sham hearts are summarized in Figure 3D. In contrast to its effect in Sham myocytes, C3SD had no effect on I_{Ca} density in intact CAL myocytes (Figs. 3E left panel, 3F and 3H). Nor did C3SD have any effect on I_{Ca} in DT CAL myocytes (Figs. 3E right panel, 3G and 3H). Thus, there appears to be no Cav-3 dependent regulation of I_{Ca} at the surface membrane in either Sham or CAL myocytes. However, there does appear to be Cav-3 dependent stimulation of I_{Ca} at the t-tubules of Sham myocytes, which is absent in CAL cells.

The effect of CAL on the response to H-89 in the absence and presence of C3SD

Since it has been suggested that Cav-3 dependent stimulation of t-tubular I_{Ca} is via a PKA-dependent mechanism (5), we investigated the effect of the PKA inhibitor H-89 on I_{Ca} density

following CAL, and the effect of C3SD on the response to H-89. Inhibition of PKA (20 μmol/L H-89) decreased I_{Ca} in untreated and C3SD-treated Sham myocytes, indicating constitutive stimulation of I_{Ca} by PKA that did not require Cav-3 (Figs. 4A – C). Moreover, there was no difference in the I_{Ca} density-voltage relations of untreated and C3SD-treated cells in the presence of H-89 (Fig. 4B), demonstrating that the effects of H-89 and C3SD-treatment were not summative. Thus, in the presence of PKA inhibition, treatment with C3SD peptide was without effect on I_{Ca} density, indicating that PKA activity was required for the constitutive regulation of I_{Ca} by Cav-3 in Sham myocytes. Similarly, H-89 decreased I_{Ca} density to the same level in both untreated and C3SD-treated CAL myocytes, indicating constitutive regulation of I_{Ca} by PKA (Figs. 4D – F). C3SD was without effect on I_{Ca} density in either the absence or presence of H-89 (Figs. 4E and 4F). These data show that in Sham myocytes there is constitutive stimulation of I_{Ca} by PKA that is mediated both via Cav-3-dependent (localized to the t-tubule membrane) and Cav-3-independent mechanisms. Although the constitutive regulation by Cav-3 was lost in CAL myocytes, constitutive regulation of I_{Ca} via PKA remained.

The effect of detubulation on the constitutive regulation of I_{Ca} by PKA

To investigate further the site of constitutive PKA-dependent regulation, the response to H-89 was determined in DT myocytes. I_{Ca} density was reduced by H-89 in both intact and DT Sham myocytes (Figs. 5A – C). I_{Ca} density was also reduced by DT both in the presence or absence of PKA inhibition (Fig. 5C). H-89 also reduced I_{Ca} density in intact and DT myocytes from CAL hearts (Figs. 5D – F). However, in contrast to Sham myocytes, in CAL, I_{Ca} density was similar in intact and DT myocytes either in the presence or absence of PKA inhibition (Fig. 5F).

The calculated current densities at the cell surface and in the t-tubule membrane before and

after inhibition of PKA are shown in Figure 6. These data show that in Sham myocytes, without inhibition of PKA, I_{Ca} density was significantly greater in the t-tubule membrane than at the cell surface, consistent with previous reports (5, 6, 16). In contrast, in CAL myocytes there was no difference in I_{Ca} density between t-tubule and surface membranes (Fig. 6B). Inhibition of PKA caused a broadly similar fractional decrease in I_{Ca} at the surface membrane in both Sham and CAL myocytes, so that surface membrane I_{Ca} remained larger in CAL than in Sham myocytes. Thus, constitutive stimulation of basal I_{Ca} by PKA at the cell surface was similar in the two cell types. H-89 also decreased t-tubular I_{Ca} density in both cell types so that it was smaller in CAL than in Sham myocytes. However, following inhibition of PKA, I_{Ca} density remained higher at the t-tubules than in the surface membrane in Sham myocytes whereas in CAL myocytes, I_{Ca} density was *smaller* at the t-tubules than at the surface membrane. Thus, it appears not only that I_{Ca} redistributes from the t-tubules to the cell surface in heart failure but also that constitutive regulation of t-tubular I_{Ca} by PKA is increased in these cells (*cf*. Fig. 6A and Fig. 6B).

DISCUSSION

This study presents two novel findings regarding the regulation of I_{Ca} in heart failure: Firstly, stimulation of I_{Ca} by β_2-adrenoceptors, but not by adenylyl cyclase/PKA, is localized to the t-tubules in Sham myocytes, and redistributes to the cell surface following CAL. Secondly, it demonstrates constitutive stimulation of I_{Ca} by PKA in Sham myocytes that is mediated both via Cav-3-dependent (at the t-tubules) and Cav-3-independent mechanisms, whereas in CAL myocytes, constitutive regulation by Cav-3 is lost although that via PKA remains at both sites. Thus, the study advances previous findings from our laboratory that Cav-3 plays a role in the regulation of I_{Ca} at the t-tubule by PKA and β_2-adrenoceptors in normal myocytes (5, 9) and that I_{Ca} is redistributed from the t-tubules to the surface sarcolemma in CAL-induced heart failure (6). Interestingly, although constitutive PKA-dependent stimulation of I_{Ca} at the cell surface appeared to be the same in both Sham and CAL myocytes, constitutive stimulation of t-tubular I_{Ca} appeared to *increase* in CAL myocytes, helping to maintain t-tubular I_{Ca}. Figure 7 shows schematic diagrams illustrating the regulation of I_{Ca} by β_2-adrenoceptors, Cav-3 and PKA in normal cells (panel A) and in heart failure (panel B).

Localization of I_{Ca} Regulation by PKA in Sham myocytes

The $Ca_v1.2$ pore-forming α-subunit of ventricular LTCCs has been shown to be colocalized with Cav-3, adenylyl cyclase, PKA and the β_2-adrenoceptor (1). Stimulation of β_2-adrenoceptors in cardiac myocytes activates adenylyl cyclase, causing a local increase of cyclic AMP, activation of PKA and thereby phosphorylation and stimulation of co-localized LTCCs (1). The present data show that β_2-adrenoceptor stimulation of I_{Ca} in Sham myocytes occurs predominantly at the t-tubules (Figure 1), although direct activation of adenylyl cyclase using forskolin increased I_{Ca} at both the t-tubular and surface membranes (Figure 2). Thus, in normal myocytes, adenylyl cyclase and the downstream pathway is present at both

294 the t-tubular and surface membranes, but the β_2-adrenoceptor is present only at the t-tubules,
295 consistent with previous work showing t-tubular localization of β_2-adrenoceptor signaling in
296 normal ventricular myocytes (27). Pretreatment with the C3SD peptide decreased basal I_{Ca} at
297 the t-tubules but not at the surface membrane in Sham myocytes (Figure 3), showing that
298 Cav-3 plays a role in the constitutive stimulation of I_{Ca} at the t-tubules, but not at the surface
299 membrane in normal cells (Fig. 7A). These data are entirely consistent with our previous
300 report in which we showed that pretreatment with C3SD abolished both the constitutive
301 regulation of I_{Ca} at the t-tubule and the response to β_2-adrenoceptors in myocytes from
302 unoperated animals (5). In contrast, inhibition of PKA using H-89 in the present study
303 decreased I_{Ca} at both the surface and t-tubule membranes, presumably reflecting the loss of
304 tonic activity of the adenylyl cyclase/cyclic AMP/PKA pathway at both the surface and t-
305 tubular membranes (Fig. 5, and summarized in Fig. 7A). Although it has been suggested that
306 H-89 may have non-specific effects independent of PKA inhibition (26), we have previously
307 shown that basal I_{Ca} was decreased by the peptide inhibitor of PKA, PKI (9). Moreover, we
308 have recently shown that H-89 was without effect on basal I_{Ca} in rat atrial myocytes from the
309 same hearts as used in the present study, demonstrating both regional differences in the role
310 of PKA in the regulation of I_{Ca} and that H-89 was without direct effect on L-type Ca^{2+}
311 channel currents *per se* (3). The regulation of basal I_{Ca} by constitutive PKA activity has also
312 been demonstrated previously in rat ventricular myocytes (4, 5, 9).
313 While the inhibitory effect of H-89 in Sham myocytes was not abolished by
314 pretreatment of the cells with C3SD, H-89 reduced basal I_{Ca} to the same mean amplitude in
315 C3SD-treated and untreated cells (Figure 4), indicating that the effects of C3SD and H-89
316 were not summative. Thus, PKA is required for the constitutive regulation of I_{Ca} by Cav-3 at
317 the t-tubules in Sham myocytes, but there is an additional Cav-3-independent constitutive
318 regulation of I_{Ca} by PKA. As basal I_{Ca} density in detubulated Sham myocytes was reduced by

H-89, but not by C3SD, it can be concluded that PKA is also involved in the constitutive regulation of I_{Ca} at the surface sarcolemma through a mechanism independent of Cav-3. Taken together, these data suggest a role for Cav-3 in co-ordinating a complex of signaling proteins including LTCC, PKA and the β_2-adrenoceptor at the t-tubule membrane in normal ventricular myocytes (1, 5, 27). While Cav-3 is important to the constitutive maintenance of I_{Ca} by PKA at the t-tubule in normal ventricular myocytes, it does not appear to be required for localizing I_{Ca} density at the t-tubule membrane because the difference in I_{Ca} density between t-tubule and surface sarcolemma was maintained following inhibition of PKA (Fig. 6A).

Regulation of I_{Ca} by PKA in CAL myocytes

In contrast to Sham myocytes, I_{Ca} increased in response to β_2 adrenergic stimulation in both intact and DT CAL myocytes (Figure 1). Moreover, C3SD had no effect on I_{Ca} in CAL myocytes (Figure 3). However, as in Sham myocytes, forskolin increased (Figure 2), and H-89 decreased (Figures 4, 5 & 6), I_{Ca} at both the surface and t-tubular membranes. The simplest explanation of these data is that the normal Cav-3-dependent localization of β_2-adrenoceptor signaling at the t-tubules is disrupted in CAL myocytes, so that the β_2-adrenoceptor is distributed across both the surface and t-tubular membranes, and can stimulate adenylyl cyclase/PKA and thus LTCCs at both sites, even without Cav-3 regulation; this is consistent with the redistribution of β_2-adrenoceptor cyclic AMP signaling in heart failure (27) and demonstrates that Cav-3 is not required for β_2-adrenoceptor stimulation of adenylyl cyclase/PKA, which are already present at both sites (Fig. 7B). Interestingly, in the presence of H-89, I_{Ca} density was similar in the t-tubular and surface membranes of CAL myocytes, suggesting that LTCCs are also redistributed in heart failure (6). The mechanisms underlying the redistribution of β_2-adrenoceptors and LTCCs away

from the t-tubules, resulting in a more uniform distribution across the cell membrane, are unclear; presumably the redistribution of Cav-3 to non-cholesterol-rich membranes in heart failure leads to a loss of Cav-3 from the t-tubules and consequent disruption of Cav-3-dependent complexes containing LTCC/adenylyl cyclase/PKA/β_2-adrenoceptors (29). Cav-3 likely plays a role in the localization of the β_2-adrenoceptor to the t-tubule so that the loss of Cav-3 regulation from the t-tubule membrane in heart failure contributes directly to the re-distribution of the receptor to the surface sarcolemma and the loss of localization of β_2-adrenoceptor signaling to the t-tubule in failing myocytes (1, 5, 27, 32). Alternatively, in principle, it is possible that β_2-adrenoceptors are more uniformly distributed between the t-tubule and surface membranes and that Cav-3 may be responsible for the localization of adenylyl cyclase/PKA signaling to the β_2-adrenoceptors in the t-tubules. Consistent with either of these proposals, treatment of normal ventricular myocytes with the C3SD peptide has been shown to antagonize β_2-adrenoceptor-mediated increases in I_{Ca} (5). Moreover, over-expression of Cav-3 restored the localization of β_2-adrenoceptor signaling to the t-tubules in failing cells, implying a direct role for Cav-3 in the localization of the receptors and/or receptor signaling to the t-tubules, presumably via binding with the scaffolding domain (32). However, the observation that zinterol stimulates I_{Ca} at the surface membrane of CAL myocytes, in which C3SD has no effect on I_{Ca}, suggests that β_2-adrenoceptor stimulation can stimulate adenylyl cyclase/PKA even without Cav-3 binding. The role of Cav-3 in the loss of t-tubular localization of β_2-adrenoceptor signaling in heart failure might be tested in future studies by investigating the effect of the C3SD peptide on the response of CAL myocytes to β_2 stimulation. On the other hand, Cav-3 does not seem to play a direct role in the localization of LTCC to the t-tubule because (i) interference of Cav-3 binding to its partners in intact Sham myocytes by treatment with the C3SD peptide had no effect on I_{Ca} in the presence of PKA inhibition (Fig. 4), indicating that PKA activity was required for the Cav-3-dependent

regulation of LTCC and (ii) PKA was not required for the concentration of I_{Ca} at the t-tubule in Sham myocytes (Fig. 4). Although Cav-3-dependent regulation of t-tubular I_{Ca} by PKA was lost in CAL myocytes, they showed an increased ratio of basal t-tubular I_{Ca} density to t-tubule I_{Ca} density in the presence of H-89, compared to Sham myocytes (CAL, basal -5.9 ± 1.6, H-89 -1.7 ± 0.8 pA/pF; Sham, basal -12.9 ± 3.0, H-89 -7.4 ± 1.6 pA/pF), indicating that the contribution of PKA to the maintenance of t-tubular I_{Ca} was augmented in heart failure. This is consistent with increased PKA-dependent regulation of basal whole-cell I_{Ca} in failing human ventricular myocytes (10). Nevertheless, the mechanism for the increased constitutive regulation of t-tubular I_{Ca} by PKA in heart failure remains unclear.

Functional implications of regulation of I_{Ca} by PKA

Previous work has shown that I_{Ca} occurs predominantly in the t-tubules, in close proximity to RyRs in the SR membrane, allowing efficient coupling between Ca entry via I_{Ca} and Ca release from the SR. The present work shows that even in the presence of PKA inhibition, I_{Ca} still occurs predominantly in the t-tubules of Sham myocytes, suggesting a higher concentration of LTCCs in the t-tubules. The observation that β_2-adrenoceptor stimulation of I_{Ca} is normally localized to the t-tubules is consistent with the importance of this site for the normal regulation of excitation-contraction coupling, and the potential detrimental effects of a whole-cell increase of cAMP.

In CAL myocytes, although there was little change in whole cell I_{Ca} density, there was redistribution of I_{Ca} so that it was more uniformly distributed across the surface and t-tubular membranes. Unless accompanied by parallel redistribution of RyRs which, to the best of our knowledge does not occur, the reduced Ca entry at the t-tubules will result in less effective coupling of Ca entry and release, and increased numbers of “orphaned” RyRs, resulting in a smaller slower Ca transient and thus contraction. However, the present work shows that

increased local constitutive stimulation of I_{Ca} by PKA helps to maintain I_{Ca} at the t-tubules, which will help ameliorate these deleterious effects.

It has been proposed that a sub-population of LTCCs in surface membrane caveolae play a role in cardiac hypertrophy (12, 24). The observation that C3SD has little effect on I_{Ca} in DT Sham or CAL myocytes suggests that Cav-3 binding has little effect on LTCC function at the cell surface, although it remains possible that downstream effects of I_{Ca} are altered.

Summary

The present study shows that Cav-3 plays a vital role in the co-ordination of PKA-dependent regulation of both basal and β_2-adrenoceptor stimulation of I_{Ca} in myocytes from healthy hearts. The co-localization by Cav-3 is lost in heart failure and both β_2-adrenoceptors and LTCC are redistributed from the t-tubular to the surface sarcolemma membranes. The role of Cav-3 in the redistribution in heart failure remains unclear but the data are consistent with a shift in Cav-3 from cholesterol-rich to non-cholesterol-rich membranes (29).

Funding

Funded by British Heart Foundation Grants PG/10/91/28644, PG/14/65/31055, and RG/12/10/29802.

FIGURE LEGENDS

Figure 1. β_2-adrenergic potentiation of I_{Ca} in Sham and CAL myocytes. **A** Representative I_{Ca} traces (elicited by step depolarization to 0 mV) recorded from intact and detubulated (DT) myocytes isolated from Sham hearts. Overlapping traces are from the same cell and recorded under control conditions and after the application of 1 μmol/L and 3 μmol/L zinterol (in the presence of 10 μmol/L atenolol). The vertical scale bar = 1 nA and the horizontal scale bar = 50 ms. **B** Time course of changes in mean normalized peak I_{Ca} (±SEM) of intact (filled symbols, n=5) and DT (open symbols, n=6) Sham myocytes during superfusion with control solution (containing 10 μmol/L atenolol) and 1 & 3 μmol/L zinterol. I_{Ca}, elicited by step depolarization to 0 mV at 0.1 Hz, was expressed as a percentage of control measured just before the application of the first concentration of zinterol. **C** Mean changes in I_{Ca} elicited by the application of 1 & 3 μmol/L zinterol to intact (filled bar, 1 μmol/L n=7; 3 μmol/L n=9) and DT (open bar, 1 μmol/L n=7; 3 μmol/L n=9] Sham myocytes. Data were subject to two-way ANOVA: β_2-agonism $p<0.001$, DT $p<0.001$; interaction $p<0.001$. * = $p<0.05$, *** = $p<0.001$; Bonferroni *post hoc* test. **D** Representative I_{Ca} traces (elicited by step depolarization to 0 mV) recorded from intact and DT myocytes isolated from CAL hearts. Conditions and scale as in A. **E** Time course of changes in mean normalized peak I_{Ca} of intact (filled symbols, n=5) and DT (open symbols, n=4) CAL myocytes during superfusion with control solution (containing 10 μmol/L atenolol) and 1 & 3 μmol/L zinterol. **F** Mean changes in I_{Ca} elicited by the application of 1 & 3 μmol/L zinterol to intact (filled bar, 1 μmol/L n=5; 3 μmol/L n=19) and DT (open bar, 1 μmol/L n=4; 3 μmol/L n=8] CAL myocytes. Data were subject to two-way ANOVA: β_2-agonism $p<0.001$, DT *ns*, interaction *ns*. ** = $p<0.01$, *** = $p<0.001$; Bonferroni *post hoc* test.

Figure 2. Increase in I_{Ca} through direction activation of adenylyl cyclase in Sham and CAL myocytes. **A** Representative I_{Ca} traces (elicited by step depolarization to 0 mV) recorded in the absence and presence of forskolin (10 μmol/L and 0.5 mmol/L $CaCl_2$) from intact and DT myocytes isolated from Sham hearts. Overlapping traces are taken from the same myocytes under control conditions and after 3 min perfusion with forskolin (FSK). Vertical scale bar = 2 pA/pF and horizontal scale bar = 100 ms. **B** Mean I_{Ca} density-voltage relationships from intact (circles, n=12) and DT (squares, n=14) Sham myocytes in the absence (open symbols) and presence (filled symbols) of FSK. *ns*, p>0.05, *, p<0.05; two-way ANOVA with Bonferroni *post hoc* test, intact vs DT cells. **C** The effect of FSK on peak I_{Ca} density (elicited at -10 mV) recorded in intact and DT Sham myocytes. Data were subject to two-way ANOVA: FSK p<0.001, DT p<0.01, interaction *ns*. *** = p<0.001; Bonferroni *post hoc* test. **D** Representative I_{Ca} traces recorded in the absence and presence of FSK (10 μmol/L and 0.5 mmol/L $CaCl_2$) from intact and DT myocytes isolated from CAL hearts. Conditions and scale as in A. **E** Mean I_{Ca} density-voltage relationships from intact (circles, n=18) and DT (squares, n=12) CAL myocytes in the absence (open symbols) and presence (filled symbols) of FSK. *ns*, p>0.05, *, two-way ANOVA with Bonferroni *post hoc* test, intact vs DT cells. **F** The effect of FSK on peak I_{Ca} density (elicited at -10 mV) recorded in intact and DT CAL myocytes. Data were subject to two-way ANOVA: FSK p<0.001, DT p<0.01, interaction *ns*. *** = p<0.001; Bonferroni *post hoc* test.

Figure 3. Constitutive regulation of basal I_{Ca} by caveolin-3. **A** Representative I_{Ca} traces recorded from intact and DT myocytes isolated from Sham hearts. Overlapping traces are taken from different myocytes that had either undergone incubation with the peptide C3SD (1 µmol/L) or were untreated. The vertical scale bar = 2 pA/pF and the horizontal scale bar = 100 ms. **B** Mean I_{Ca} density-voltage relations from untreated intact Sham cells (open circles, n=16) and intact Sham cells treated with the C3SD peptide (filled circles, n=16). **, p<0.01; two-way ANOVA with Bonferroni *post hoc* test, untreated vs C3SD-treated cells. **C** Mean I_{Ca} density-voltage relations from untreated Sham DT cells (open squares, n=20) and Sham DT cells treated with the C3SD peptide (filled squares, n=10). *ns*, p>0.05; two-way ANOVA with Bonferroni *post hoc* test, untreated vs C3SD treated cells. **D** The effect of C3SD on peak I_{Ca} density (elicited at 0 mV) recorded from Intact and DT, Sham myocytes. Data were subject to two-way ANOVA: C3SD *ns*, DT p<0.001, interaction p<0.01. ** = p<0.01, *** = p<0.001; Bonferroni *post hoc* test. **E** Representative I_{Ca} traces recorded from intact and DT myocytes isolated from CAL hearts. Conditions and scale as in A and overlapping traces are taken from different myocytes that had either undergone incubation with the peptide C3SD (1 µmol/L) or were untreated. **F** Mean I_{Ca} density-voltage relations from untreated intact CAL cells (open circles, n=14) and intact CAL cells treated with the C3SD peptide (filled circles, n=15). *ns*, p>0.05; two-way ANOVA with Bonferroni *post hoc* test, untreated vs C3SD treated cells. **G** Mean I_{Ca} density-voltage relations from untreated DT CAL cells (open squares, n=22) and DT CAL cells treated with the C3SD peptide (filled squares, n=7). *ns*, p>0.05; two-way ANOVA with Bonferroni *post hoc* test, untreated vs C3SD treated cells. **H** The effect of C3SD on peak I_{Ca} density (elicited at 0 mV) recorded from Intact and DT, CAL myocytes. Data were subject to two-way ANOVA: C3SD *ns*, DT *ns*, interaction *ns*.

Figure 4. The role of PKA in caveolin-3-dependent regulation of basal I_{Ca} in Sham and CAL myocytes. **A** Representative I_{Ca} traces recorded from intact untreated (Control) and C3SD-treated (C3SD) myocytes isolated from Sham hearts. Overlapping traces are taken from the same myocytes before and after the application of the PKA inhibitor H-89 (20 μmol/L). The vertical scale bar = 2 pA/pF and the horizontal scale bar = 100 ms. **B** Mean I_{Ca}-density voltage-relationship curves recorded from intact myocytes isolated from Sham hearts that were either untreated (open symbols, n=16) or treated with C3SD (filled symbols, n=16) before (circles) and after (squares) the application of H-89. The control data is the same as that shown in Figure 3B. ***, $p<0.001$; two-way ANOVA with Bonferroni *post hoc* test absence vs presence of H-89. **C** The effect of PKA inhibition on mean peak I_{Ca} density (elicited at 0 mV) in Sham myocytes that were untreated (open bars) or treated (filled bars) with C3SD. Data were subject to two-way ANOVA: C3SD *ns*, H-89 $p<0.001$, interaction *ns*. * = $p<0.05$, ** = $p<0.01$, *** = $p<0.001$, Bonferroni *post hoc* test. **D** Representative I_{Ca} traces recorded from untreated and C3SD-treated myocytes isolated from CAL hearts before and after the application of the PKA inhibitor H-89 (20 μmol/L). Conditions and scale as A. **E** Mean I_{Ca}-density voltage relationship curves recorded from intact myocytes isolated from CAL hearts that were either untreated (open symbols, n=14) or treated with C3SD (filled symbols, n=15) before (circles) and after (squares) the application of H-89. The control data is the same as that shown in Figure 3F. ***, $p<0.001$; two-way ANOVA with Bonferroni *post hoc* test absence vs presence of H-89. **F** The effect of PKA inhibition on mean peak I_{Ca} density (elicited at 0 mV) in CAL myocytes that were treated (filled bars) or untreated (open bars) with C3SD. Data were subject to two-way ANOVA: C3SD *ns*, H-89 $p<0.001$, interaction *ns*. *** = $p<0.001$; Bonferroni *post hoc* test.

Figure 5. The localization of PKA-dependent regulation of basal I_{Ca} in Sham and CAL myocytes. **A** Representative I_{Ca} traces recorded from intact and DT myocytes isolated from Sham hearts. Overlapping traces are taken from the same myocytes before and after the application of the PKA inhibitor H-89 (20 µmol/L). The vertical scale bar = 2 pA/pF and the horizontal scale bar = 100 ms. **B** Mean I_{Ca}-density voltage-relationship curves recorded from myocytes isolated from Sham hearts that were either intact (circles, n=17) or DT (squares, n=8) before (open symbols) and after (filled symbols) the application of H-89. ***, p<0.001; two-way ANOVA with Bonferroni *post hoc* test control vs H-89. **C** The effect of PKA inhibition on mean peak I_{Ca} density (elicited at 0 mV) in intact or DT Sham myocytes under control conditions (open bars) or after PKA inhibition (H-89, filled bars). Data were subject to two-way ANOVA: H-89 p<0.001, DT p<0.001, interaction p<0.05. *** = p<0.001; Bonferroni *post hoc* test. **D** Representative I_{Ca} traces recorded from intact and DT myocytes isolated from CAL hearts; overlapping traces are taken from the same myocytes before and after the application of the PKA inhibitor H-89. Conditions and scale as A. **E** Mean I_{Ca}-density voltage-relationship curves recorded from myocytes isolated from CAL hearts that were either intact (circles, n=14) or DT (squares, n=9) before (open symbols) and after (filled symbols) the application of H-89. ***, p<0.001; two-way ANOVA with Bonferroni post hoc test control vs H-89. **F** The effect of PKA inhibition on mean peak I_{Ca} density (elicited at 0 mV) in intact or DT Sham myocytes under control conditions (open bars) or after PKA inhibition (H-89, filled bars). Data were subject to two-way ANOVA: H-89 p<0.001, DT *ns*, interaction *ns*. *** = p<0.001; Bonferroni *post hoc* test.

Figure 6. A Mean I_{Ca} density at 0 mV measured in intact ('total cell membrane') and detubulated cells ('Surface membrane') and calculated at the t-tubules ('t-tubule membrane') for Sham myocytes. Correction for incomplete detubulation has been applied (see Methods). Open (left) columns are in control conditions and filled (right) columns are in the presence of H-89. **B** Mean I_{Ca} density at 0 mV measured in intact ('total cell membrane') and detubulated cells ('Surface membrane') and calculated at the t-tubules ('t-tubule membrane') for CAL myocytes. Correction for incomplete detubulation has been applied (see Methods). Open (left) columns are in control conditions and filled (right) columns are in the presence of H-89. *p<0.05, **p<0.01, Student's t test.

Figure 7. A schematic summarizing the role of caveolin-3 (Cav-3) in the regulation of I_{Ca} in normal ventricular myocytes and in heart failure. **A** Regulation of I_{Ca} in normal cardiac myocytes. LTCC density is greatest in the t-tubules, where Cav-3 co-ordinates a signaling domain involving β_2-adrenoceptors (β_2AR), adenylyl cyclase (Ad Cyc), PKA and the LTCC α_{1c}-subunit, $Ca_v1.2$. β_2AR coupled with LTCC are located exclusively in the t-tubules. Ad Cyc, PKA and $Ca_v1.2$ are also located outside of Cav-3 signaling domains, both within and without t-tubules. Activation of Ad Cyc, either via β_2AR or directly, augments LTCC activity through production of cAMP. **B** Remodeling of I_{Ca} regulation in heart failure. The Cav-3 signaling complex is disrupted. β_2AR are located both within the t-tubules and on the surface sarcolemma. LTCC density is more evenly distributed between t-tubules and surface sarcolemma. The role of Cav-3 in the regulation of I_{Ca} is lost in heart failure. The schematic represents the simplest explanation of the data. Other mechanisms are possible; for example, β_2AR may be located in both the cell surface and t-tubule membranes in normal cardiac myocytes but the coupling of β_2AR with LTCC confined to the t-tubules.

REFERENCES

1. **Balijepalli RC, Foell JD, Hall DD, Hell JW, and Kamp TJ**. Localization of cardiac L-type Ca^{2+} channels to a caveolar macromolecular signaling complex is required for β_2-adrenergic regulation. *Proc Natl Acad Sci USA* 103: 7500-7505, 2006.
2. **Beuckelmann DJ, and Wier WG**. Mechanism of release of calcium from sarcoplasmic reticulum of guinea-pig cardiac cells. *J Physiol (Lond)* 405: 233-255, 1988.
3. **Bond RC, Bryant SM, Watson JJ, Hancox JC, Orchard CH, and James AF**. Reduced density and altered regulation of rat atrial L-type Ca^{2+} current in rat heart failure. *Am J Physiol Heart Circ Physiol* 312: H384-H391, 2017.
4. **Bracken N, ElKadri M, Hart G, and Hussain M**. The role of constitutive PKA-mediated phosphorylation in the regulation of basal I_{Ca} in isolated rat cardiac myocytes. *Br J Pharmacol* 148: 1108-1115, 2006.
5. **Bryant S, Kimura TE, Kong CHT, Watson JJ, Chase A, Suleiman MS, James AF, and Orchard CH**. Stimulation of I_{Ca} by basal PKA activity is facilitated by caveolin-3 in cardiac ventricular myocytes. *J Mol Cell Cardiol* 68: 47-55, 2014.
6. **Bryant SM, Kong CHT, Watson J, Cannell MB, James AF, and Orchard CH**. Altered distribution of I_{Ca} impairs Ca release at the t-tubules of ventricular myocytes from failing hearts. *J Mol Cell Cardiol* 86: 23-31, 2015.
7. **Calaghan S, and White E**. Caveolae modulate excitation-contraction coupling and β_2-adrenergic signalling in adult rat ventricular myocytes. *Cardiovasc Res* 69: 816-824, 2006.
8. **Cannell MB, Berlin JR, and Lederer WJ**. Effect of membrane potential changes on the calcium transient in single rat cardiac muscle cells. *Science* 238: 1419-1423, 1987.
9. **Chase A, Colyer J, and Orchard CH**. Localised Ca channel phosphorylation modulates the distribution of L-type Ca current in cardiac myocytes. *J Mol Cell Cardiol* 49: 121-131, 2010.
10. **Chen X, Piacentino V, Furukawa S, Goldman B, Margulies KB, and Houser SR**. L-Type Ca^{2+} Channel Density and Regulation Are Altered in Failing Human Ventricular Myocytes and Recover After Support With Mechanical Assist Devices. *Circ Res* 91: 517-524, 2002.
11. **Chijiwa T, Mishima A, Hagiwara M, Sano M, Hayashi K, Inoue T, Naito K, Toshioka T, and Hidaka H**. Inhibition of forskolin-induced neurite outgrowth and protein phosphorylation by a newly synthesized selective inhibitor of cyclic AMP-dependent protein kinase, N-[2-(p-bromocinnamylamino)ethyl]-5-isoquinolinesulfonamide (H-89), of PC12D pheochromocytoma cells. *J Biol Chem* 265: 5267-5272, 1990.
12. **Correll RN, Pang C, Finlin BS, Dailey AM, Satin J, and Andres DA**. Plasma Membrane Targeting Is Essential for Rem-mediated Ca^{2+} Channel Inhibition. *J Biol Chem* 282: 28431-28440, 2007.
13. **Couet J, Li S, Okamoto T, Ikezu T, and Lisanti MP**. Identification of Peptide and Protein Ligands for the Caveolin-scaffolding Domain. *J Biol Chem* 272: 6525-6533, 1997.
14. **Farrance I, and Frenkel R**. Uncertainty of Measurement: A Review of the Rules for Calculating Uncertainty Components through Functional Relationships. *Clin Biochem Rev* 33: 49-75, 2012.
15. **Feron O, Dessy C, Opel DJ, Arstall MA, Kelly RA, and Michel T**. Modulation of the Endothelial Nitric-oxide Synthase-Caveolin Interaction in Cardiac Myocytes: IMPLICATIONS FOR THE AUTONOMIC REGULATION OF HEART RATE. *J Biol Chem* 273: 30249-30254, 1998.
16. **Gadeberg HC, Bryant SM, James AF, and Orchard CH**. Altered Na/Ca exchange distribution and activity in ventricular myocytes from failing hearts. *Am J Physiol* 310: H262-H268, 2016.
17. **Hidaka H, and Kobayashi R**. Pharmacology of Protein Kinase Inhibitors. *Annu rev Pharmacol Toxicol* 32: 377-397, 1992.
18. **Hong T, and Shaw RM**. Cardiac T-Tubule Microanatomy and Function. *Physiol Rev* 97: 227-252, 2017.

19. **Horiuchi-Hirose M, Kashihara T, Nakada T, Kurebayashi N, Shimojo H, Shibazaki T, Sheng X, Yano S, Hirose M, Hongo M, Sakurai T, Moriizumi T, Ueda H, and Yamada M**. Decrease in the density of t-tubular L-type Ca^{2+} channel currents in failing ventricular myocytes. *Am J Physiol* 300: H978-H988, 2011.
20. **Isenberg G, and Klockner U**. Calcium tolerant ventricular myocytes prepared by preincubation in a "KB medium". *Pflugers Archiv* 395: 6-18, 1982.
21. **Kawai M, Hussain M, and Orchard CH**. Excitation-contraction coupling in rat ventricular myocytes after formamide-induced detubulation. *Am J Physiol* 277: H603-H609, 1999.
22. **Lyon AR, Nikolaev VO, Miragoli M, Sikkel MB, Paur H, Benard L, Hulot J-S, Kohlbrenner E, Hajjar RJ, Peters NS, Korchev YE, Macleod KT, Harding SE, and Gorelik J**. Plasticity of Surface Structures and β_2-Adrenergic Receptor Localization in Failing Ventricular Cardiomyocytes During Recovery From Heart Failure. *Circ Heart Fail* 5: 357-365, 2012.
23. **MacDougall DA, Agarwal SR, Stopford EA, Chu H, Collins JA, Longster AL, Colyer J, Harvey RD, and Calaghan S**. Caveolae compartmentalise β_2-adrenoceptor signals by curtailing cAMP production and activating phosphatase in the sarcoplasmic reticulum of the adult ventricular myocyte. *J Mol Cell Cardiol* 52: 388-400, 2012.
24. **Makarewich CA, Correll RN, Gao H, Zhang H, Yang B, Berretta RM, Rizzo V, Molkentin JD, and Houser SR**. A Caveolae-Targeted L-Type Ca^{2+} Channel Antagonist Inhibits Hypertrophic Signaling Without Reducing Cardiac Contractility / Novelty and Significance. *Circ Res* 110: 669-674, 2012.
25. **Mobley BA, and Page E**. The surface area of sheep cardiac Purkinje fibres. *J Physiol (Lond)* 220: 547-563, 1972.
26. **Murray AJ**. Pharmacological PKA Inhibition: All May Not Be What It Seems. *Sci Signal* 1: re4-, 2008.
27. **Nikolaev VO, Moshkov A, Lyon AR, Miragoli M, Novak P, Paur H, Lohse MJ, Korchev YE, Harding SE, and Gorelik J**. β_2-Adrenergic Receptor Redistribution in Heart Failure Changes cAMP Compartmentation. *Science* 327: 1653-1657, 2010.
28. **Orchard CH, Pasek M, and Brette F**. The role of mammalian cardiac t-tubules in excitation-contraction coupling: experimental and computational approaches. *Exp Physiol* 94: 509-519, 2009.
29. **Ratajczak P, Damy T, Heymes C, Oliviéro P, Marotte F, Robidel E, Sercombe R, Boczkowski J, Rappaport L, and Samuel J-L**. Caveolin-1 and -3 dissociations from caveolae to cytosol in the heart during aging and after myocardial infarction in rat. *Cardiovasc Res* 57: 358-369, 2003.
30. **Rybin VO, Xu X, Lisanti MP, and Steinberg SF**. Differential Targeting of β-Adrenergic Receptor Subtypes and Adenylyl Cyclase to Cardiomyocyte Caveolae: A MECHANISM TO FUNCTIONALLY REGULATE THE cAMP SIGNALING PATHWAY. *J Biol Chem* 275: 41447-41457, 2000.
31. **Scamps F, Mayoux E, Charlemagne D, and Vassort G**. Calcium current in single cells isolated from normal and hypertrophied rat heart: Effects of β-adrenergic stimulation. *Circ Res* 67: 199-208, 1990.
32. **Wright PT, Nikolaev VO, O'Hara T, Diakonov I, Bhargava A, Tokar S, Schobesberger S, Shevchuk AI, Sikkel MB, Wilkinson R, Trayanova NA, Lyon AR, Harding SE, and Gorelik J**. Caveolin-3 regulates compartmentation of cardiomyocyte beta2-adrenergic receptor-mediated cAMP signaling. *J Mol Cell Cardiol* 67: 38-48, 2014.
33. **You Y, Pelzer DJ, and Pelzer S**. Modulation of L-type Ca^{2+} current by fast and slow Ca^{2+} buffering in guinea pig ventricular cardiomyocytes. *Biophys J* 72: 175-187, 1997.

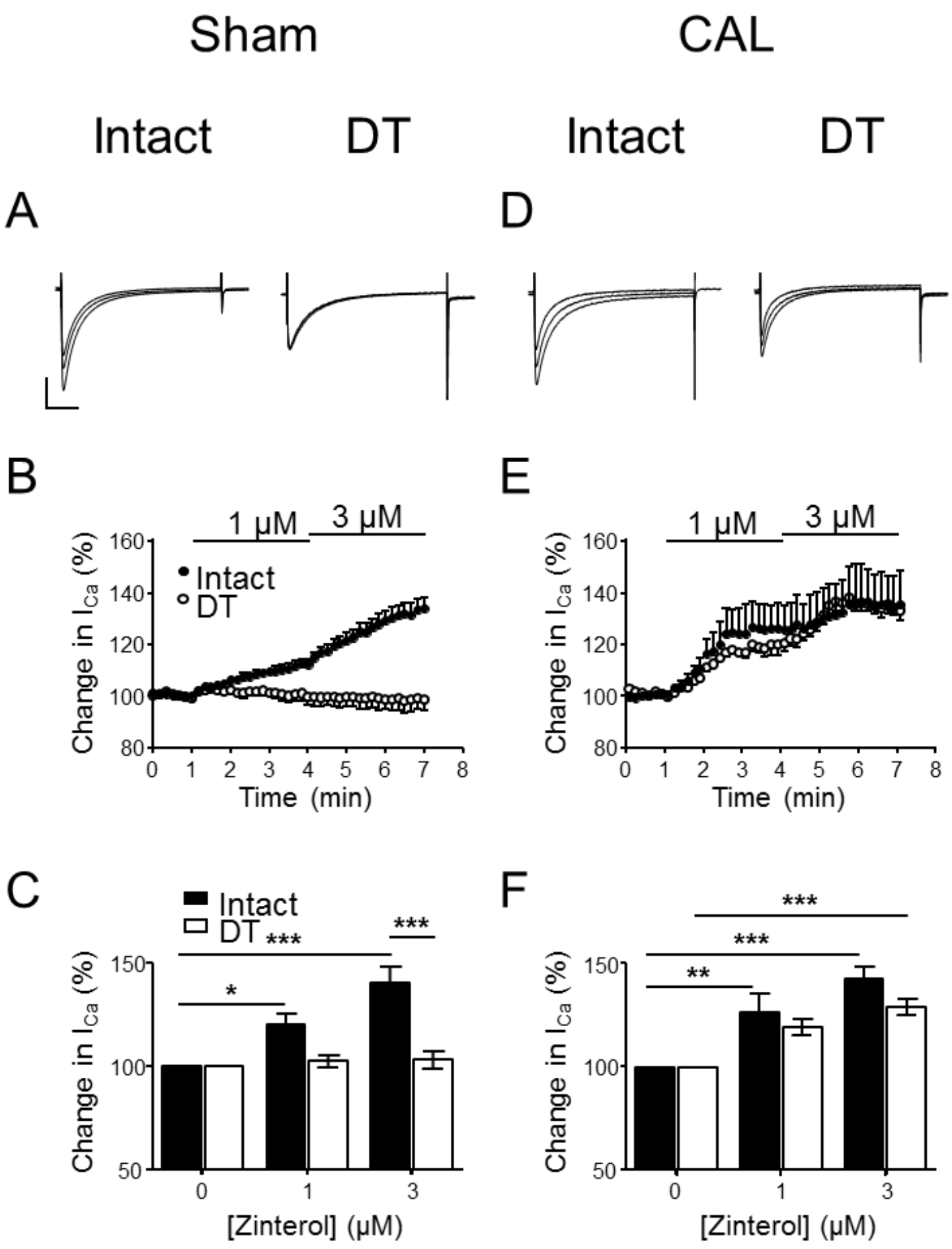
Sham
CAL
Intact
DT
Intact
DT
A
D
B
E
1 μM
3 μM
Intact
DT
Change in I_{Ca} (%)
Time (min)
C
F
Intact
DT
***
*
**
Change in I_{Ca} (%)
[Zinterol] (μM)

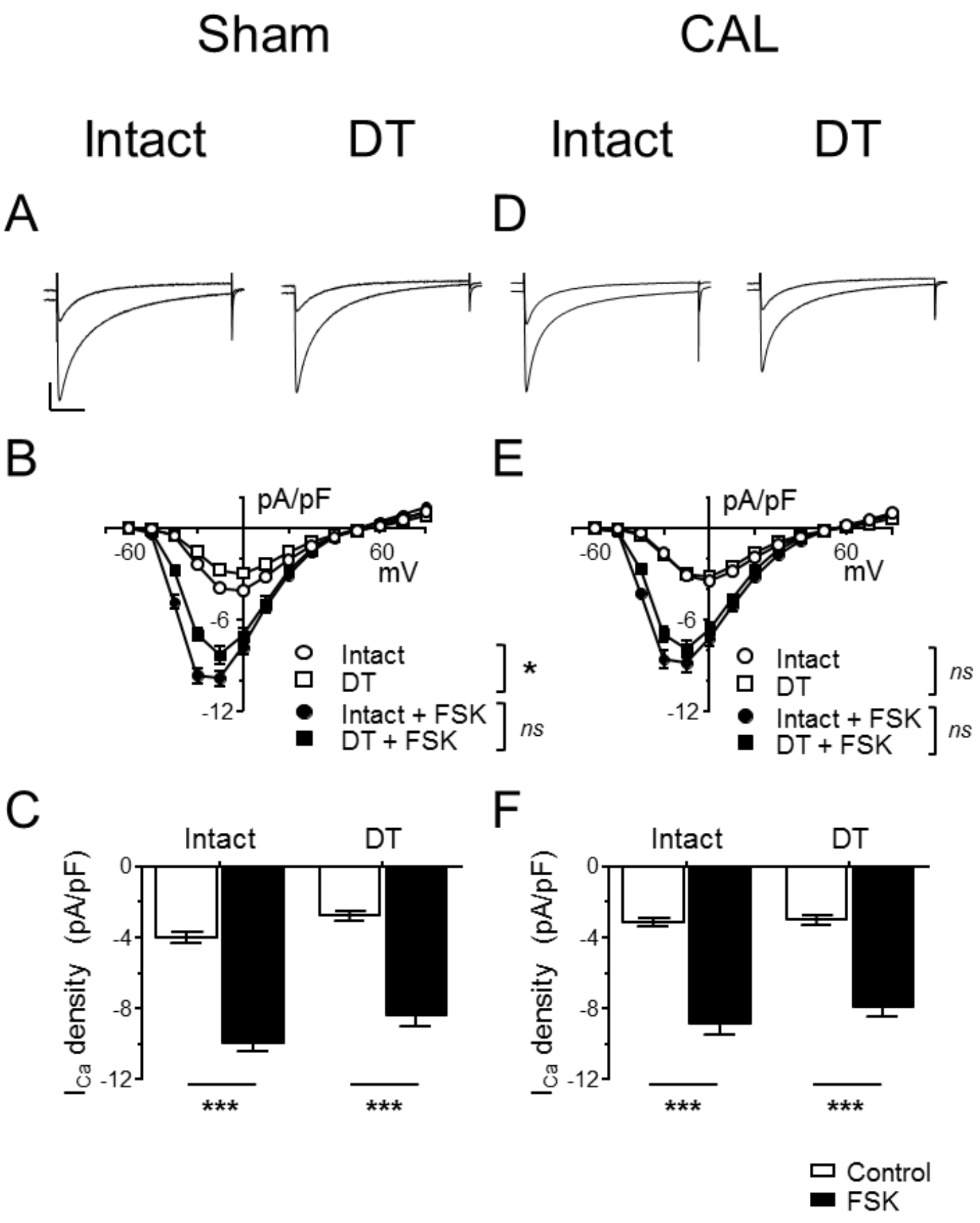
Sham
CAL
Intact
DT
Intact
DT
A
D
B
E
pA/pF
-60
60
mV
-6
-12
Intact
DT
Intact + FSK
DT + FSK
*
ns
ns
C
F
Intact
DT
0
-4
-8
-12
I_{Ca} density (pA/pF)
***
***
Control
FSK

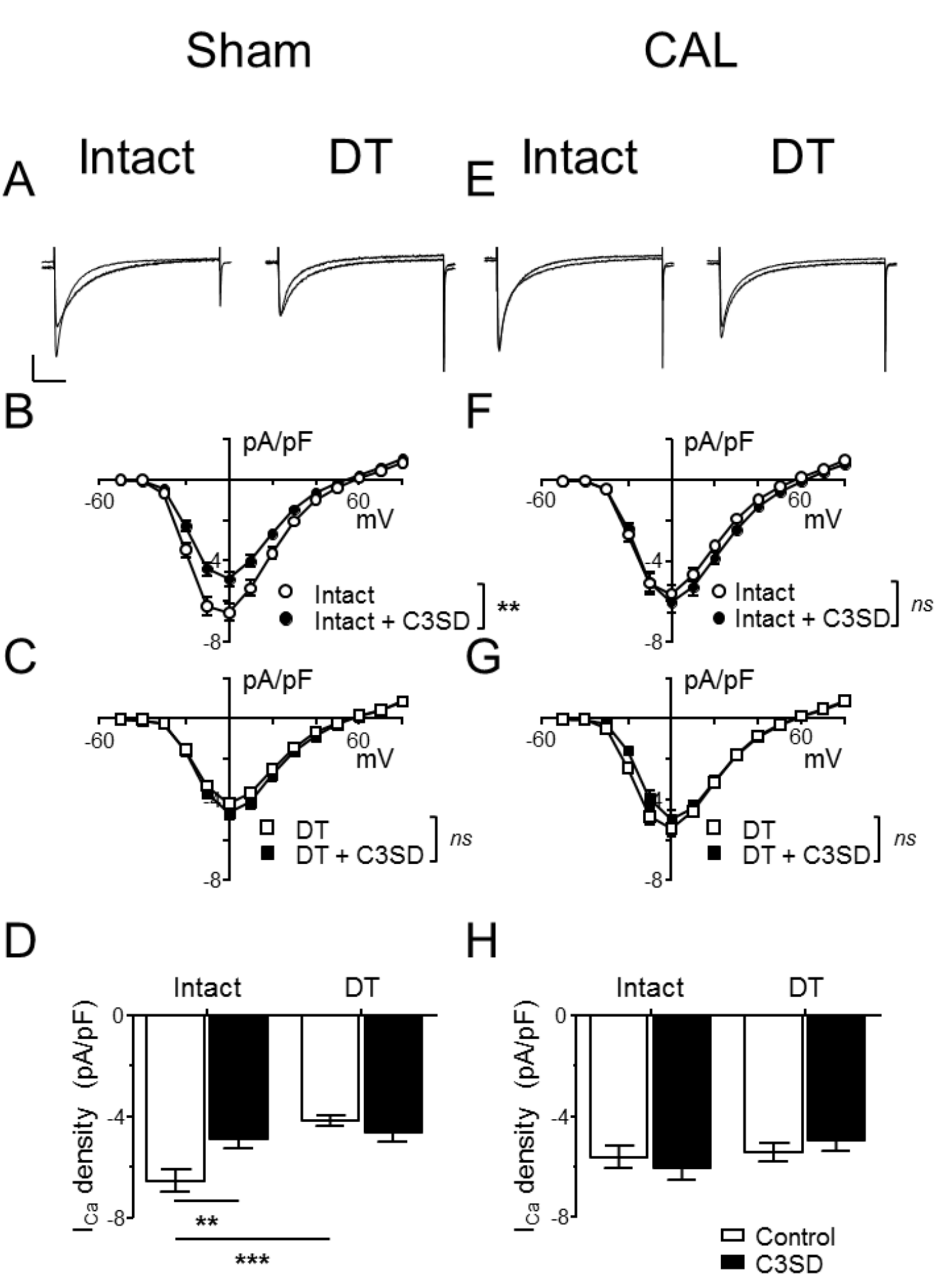
Sham
CAL
A
Intact
DT
E
Intact
DT
B
pA/pF
-60
60
mV
-4
-8
Intact
Intact + C3SD
**
F
pA/pF
-60
60
mV
-4
-8
Intact
Intact + C3SD
ns
C
pA/pF
-60
60
mV
-4
-8
DT
DT + C3SD
ns
G
pA/pF
-60
60
mV
-4
-8
DT
DT + C3SD
ns
D
Intact
DT
0
-4
-8
I_{Ca} density (pA/pF)
**
***
H
Intact
DT
0
-4
-8
I_{Ca} density (pA/pF)
Control
C3SD

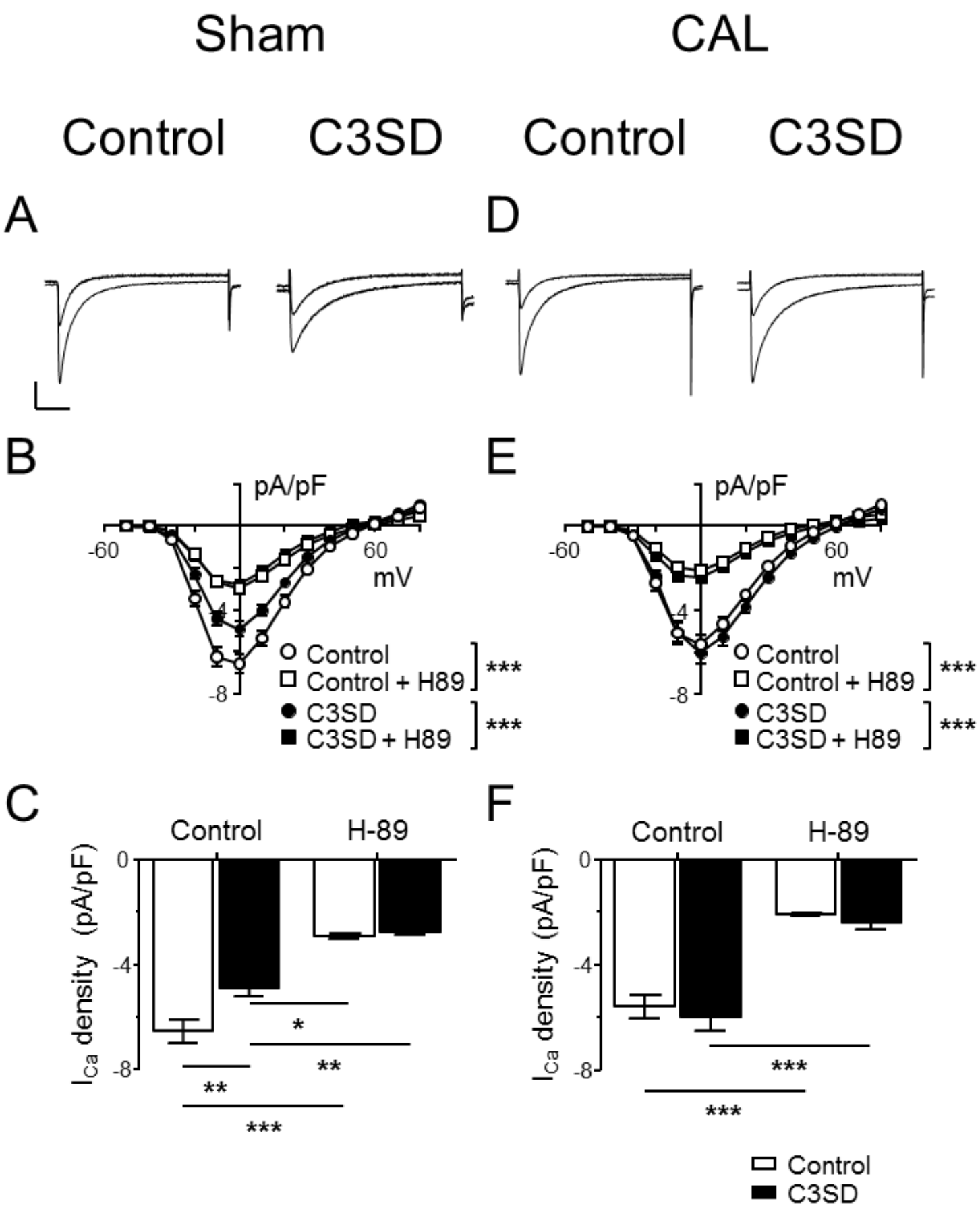
Sham
CAL
Control
C3SD
Control
C3SD
A
D
B
E
pA/pF
-60
60
mV
-4
-8
Control
Control + H89
C3SD
C3SD + H89
***
***
C
F
Control
H-89
0
-4
-8
I_{Ca} density (pA/pF)
*
**
**
***
***
Control
C3SD

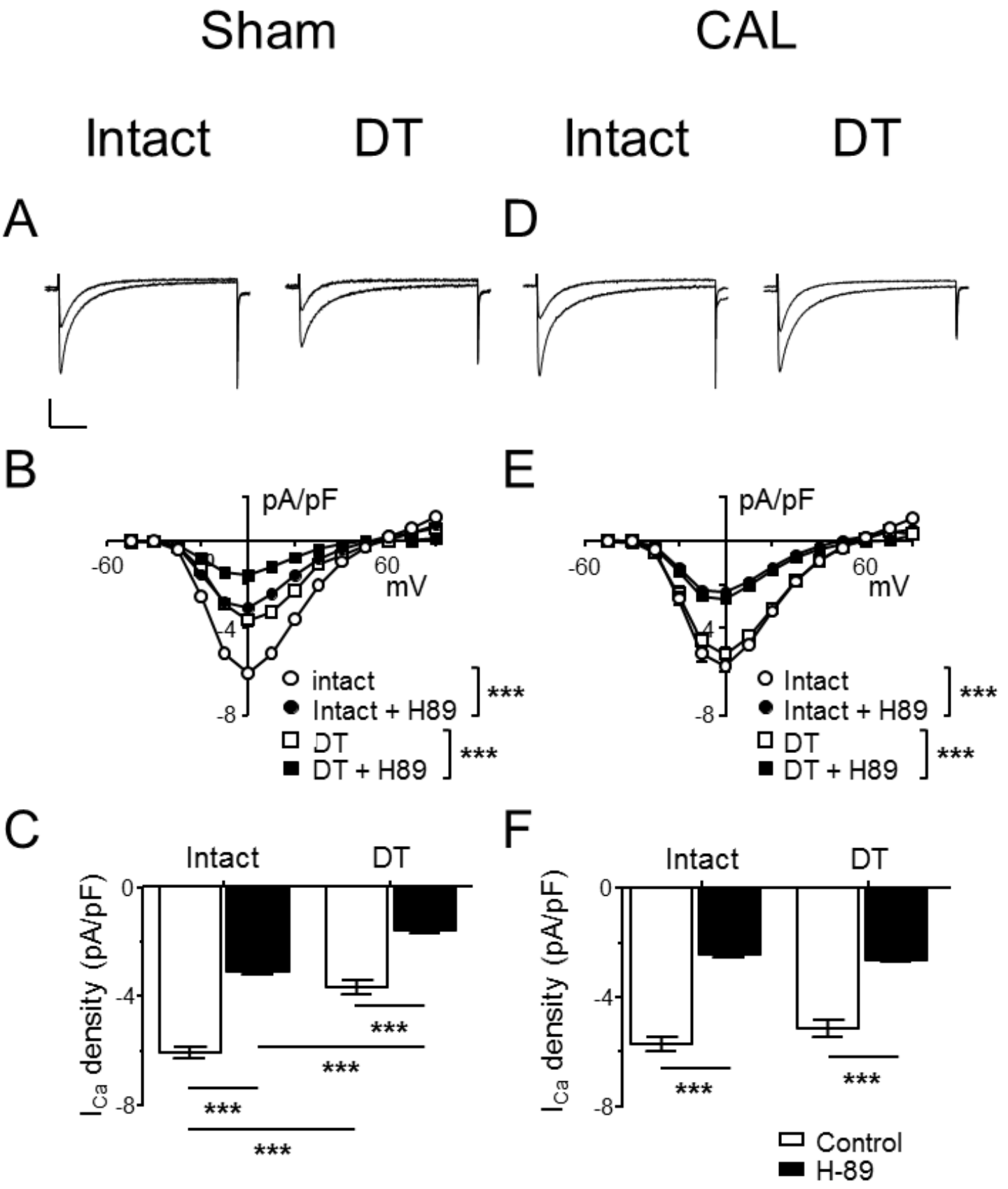
Sham
CAL
Intact
DT
Intact
DT
A
D
B
E
pA/pF
-60
60
mV
-4
-8
intact
Intact + H89
DT
DT + H89
***
***
Intact
Intact + H89
DT
DT + H89
***
***
C
F
Intact
DT
Intact
DT
0
-4
-8
I_{Ca} density (pA/pF)
***
***
***
***
Control
H-89

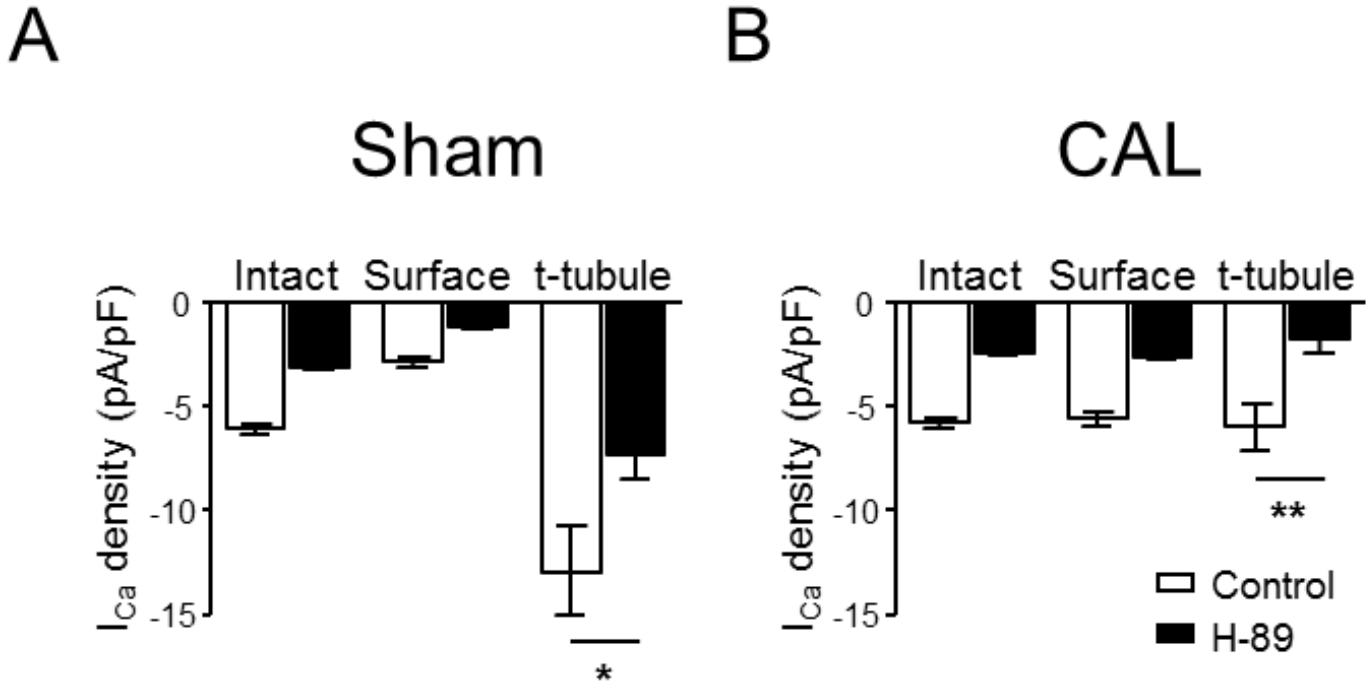
A
Sham
Intact
Surface
t-tubule
0
-5
-10
-15
I_{Ca} density (pA/pF)
*
B
CAL
Intact
Surface
t-tubule
0
-5
-10
-15
I_{Ca} density (pA/pF)
**
Control
H-89

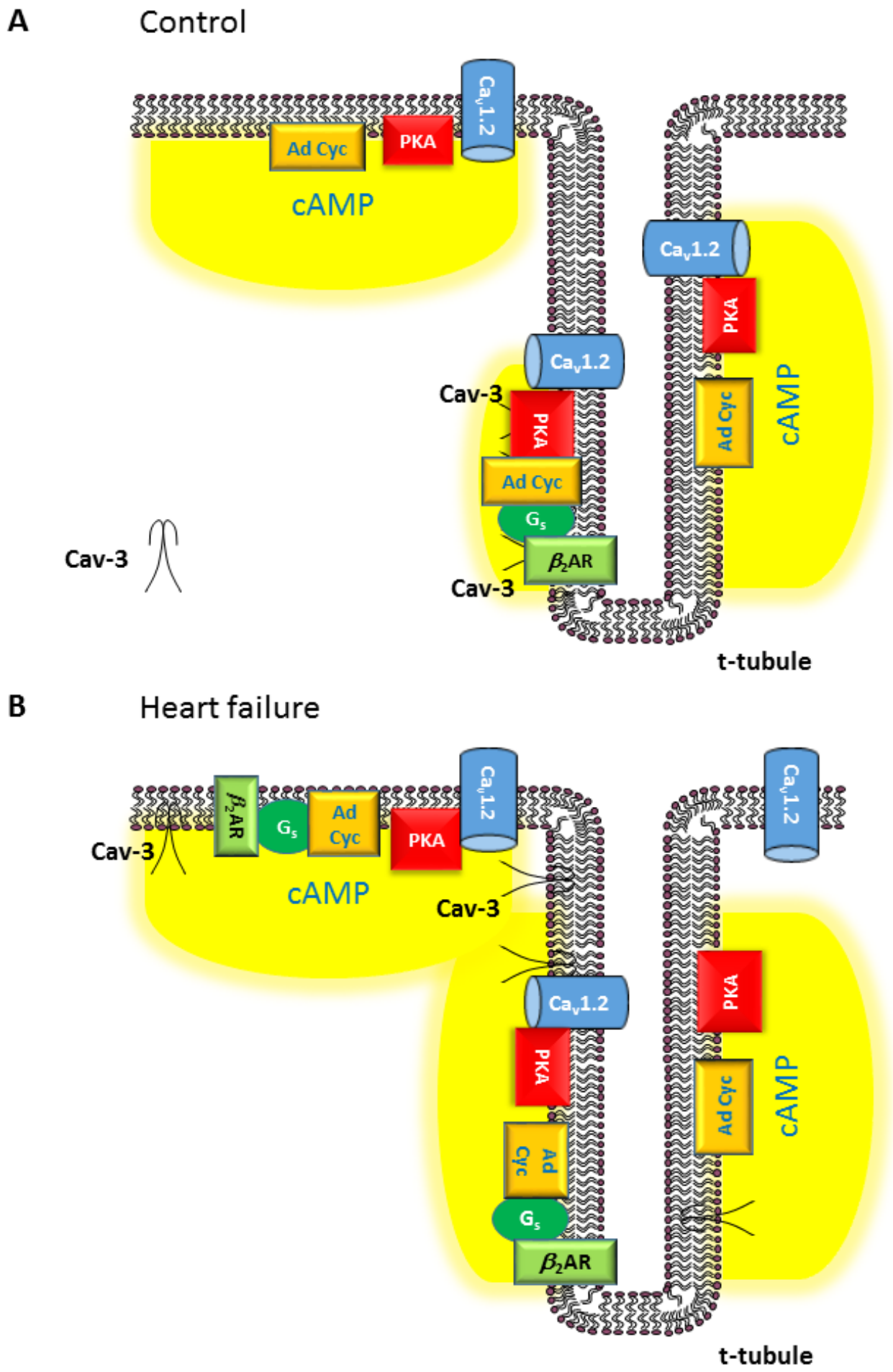
A
Control
Ad Cyc
PKA
$Ca_V1.2$
cAMP
Cav-3
Cav-3
$Ca_V1.2$
PKA
Ad Cyc
G_s
β_2AR
$Ca_V1.2$
PKA
Ad Cyc
cAMP
t-tubule
B
Heart failure
β_2AR
G_s
Ad Cyc
PKA
$Ca_V1.2$
Cav-3
cAMP
Cav-3
$Ca_V1.2$
PKA
Ad Cyc
G_s
β_2AR
$Ca_V1.2$
PKA
Ad Cyc
cAMP
t-tubule